SUPPORTING MATERIAL

Concise whole-cell modeling of $BK_{Ca}CaV$ activity controlled by local coupling and stoichiometry

F Montefusco, A Tagliavini, M Ferrante, M Pedersen

List of contents

1 Model of the 1:1 BK$_{Ca}$-CaV complex

First, we justify the product formulation for the voltage and Ca^{2+}-dependent rate constants k^- and k^+ (Eqs. 2 and 3 in the main text). We assume (i) that, for fixed Ca^{2+} concentration (Ca), BK$_{Ca}$ activity is described by a Boltzmann function, and (ii) that the slope parameter of the Boltzmann function is independent of Ca, a reasonable assumption for Ca^{2+} concentrations above 1 μM (1–3) as expected in BK$_{Ca}$-CaV complexes (2, 4). Based on assumption (i), we express the rate constants by the standard expressions

$$k^-(V, Ca) = \tilde{w}^-(Ca)e^{-w_{yx}(Ca)V}, \quad k^+(V, Ca) = \tilde{w}^+(Ca)e^{-w_{xy}(Ca)V}.$$

The open fraction of BK$_{Ca}$ channels is then

$$p_{Y\infty} = \frac{k^+(V, Ca)}{k^-(V, Ca) + k^+(V, Ca)} = \frac{1}{1 - e^{-\frac{V - V_0(Ca)}{S_0(Ca)}}},$$

where we have highlighted that in principal V_0 and S_0 depend on Ca. In particular the slope parameter is given by

$$S_0(Ca) = \frac{1}{w_{yx}(Ca) - w_{xy}(Ca)},$$

and from assumption (ii) we obtain that $w_{xy}(Ca)$ is equal to $w_{yx}(Ca)$ except from a constant independent of Ca. We make the simplifying assumption that also w_{yx} and w_{xy} are independent of Ca. Finally, writing

$$\tilde{w}^-(Ca) = w_0^- f^-(Ca), \quad \tilde{w}^+(Ca) = w_0^+ f^+(Ca)$$

we obtain Eqs. 2-5 in the main text.

We couple the two state (closed and open) model for the BK$_{Ca}$ channel (see Methods, Table S1 reporting the optimal model parameters, and Figure S1 showing a representation of the model and the fits to the data) with the three state (closed, open and inactivated or blocked) model for the CaV channel (see Methods and Table S1). Figure 1A in the main text shows a cartoon of the model of the 1:1 BK$_{Ca}$-CaV complex, where CX, OX and BX correspond to the closed state for the BK$_{Ca}$ channel (X) coupled with the closed (C), open (O) and inactivated (B) states for the CaV, respectively, and CY, OY and BY correspond to the open state for the BK$_{Ca}$ channel (Y) coupled with the closed (C), open (O) and inactivated (B) states for the CaV, respectively.

The parameters k_c^- and k_o^- (k_c^+ and k_o^+) are defined by Eq. 2 (Eq. 3) of the main text with Ca equal to Ca_c and Ca_o, respectively. Ca_c is the concentration at the BK$_{Ca}$ channel when the associated CaV is closed (or inactivated, i.e. $Ca_c = Ca_b$) and is set equal to 0.2 μM (background Ca^{2+} concentration). Ca_o is the concentration at the BK$_{Ca}$ channel when the CaV is open and is given by

$$Ca_o = \frac{i_{Ca}}{8\pi r D_{Ca} F} \exp\left[\frac{-r}{\sqrt{\frac{D_{Ca}}{k_B^+[B_{total}]}}}\right], \tag{S1}$$

where $i_{Ca} = \bar{g}_{Ca}(V - V_{Ca})$ is the single-channel Ca^{2+} current, and $r = 13$ nm the distance between CaV and BK$_{Ca}$ channels (2, 4). At $V = 0$ mV, $Ca_o \approx 19$ μM. Other parameters are given in Table S2 (2). Note that for the parameters used here (Table S1), $k_c^+ \approx 0$ (i.e., the probability of BK$_{Ca}$ opening when the CaV is closed is practically zero).
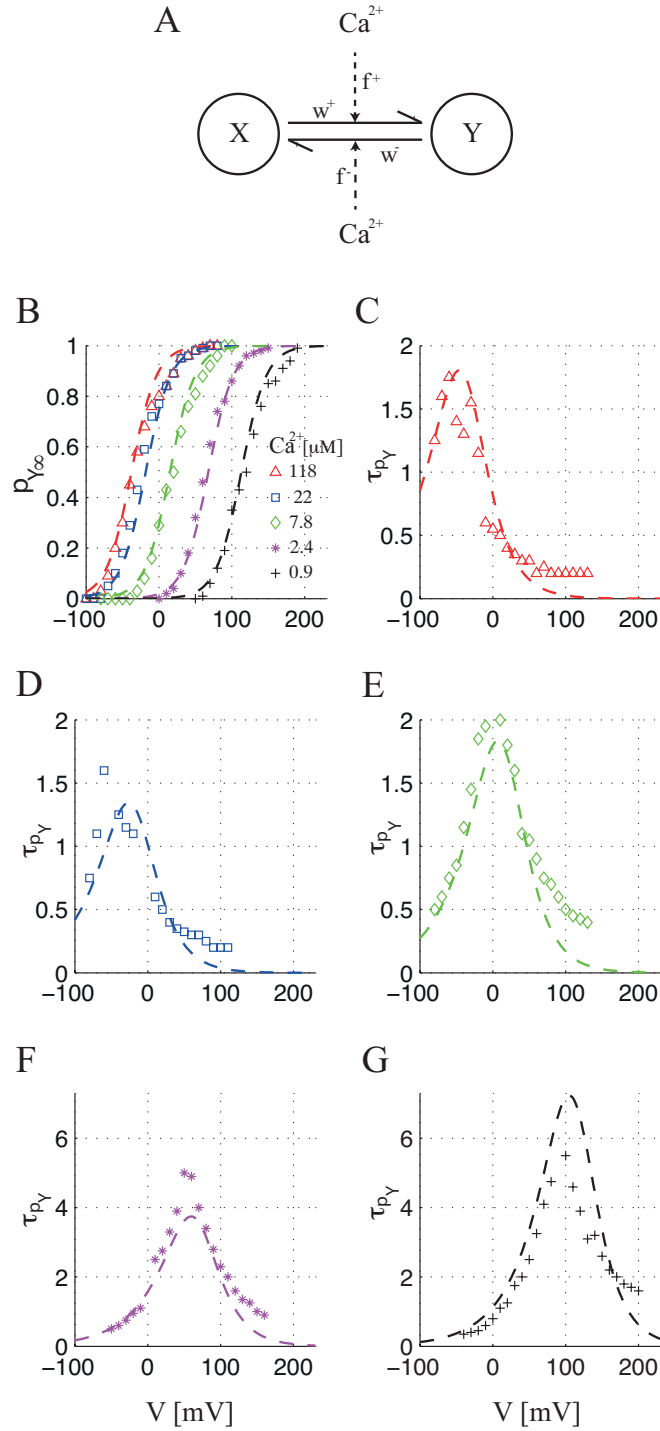
Figure S1: **BK$_{Ca}$ channel model: fit to the data.** **(A)** Schematic representation of the model, where X and Y indicate the closed and open states of the BK$_{Ca}$ channel. **(B)** Steady-state BK$_{Ca}$ open probabilities vs. voltage at different Ca^{2+} concentrations (different markers for different Ca^{2+} levels as indicated in the legend) and the corresponding fit obtained by the model (dashed lines). **(C)-(G)** Time constants (in ms) vs. voltage data at given Ca^{2+} concentrations (see legend in panel B), and the corresponding model fits (dashed lines).

Table S1: **Optimal model parameters for the BK$_{Ca}$-CaV complex.**

BK$_{Ca}$ channel model described by Eq. 1 of the main text

Parameter	Value	Unit
w_0^-	3.32	ms^{-1}
w_0^+	1.11	ms^{-1}
w_{yx}	0.022	mV^{-1}
w_{xy}	-0.036	mV^{-1}
K_{yx}	0.1	μM
K_{xy}	16.6	μM
n_{yx}	0.46	-
n_{xy}	2.33	-

CaV activation described by Eqs. 16 and 17 of the main text

Parameter	Value	Unit
α_0	1.2979	ms^{-1}
α_1	-0.0639	mV^{-1}
β_0	1.0665	ms^{-1}
β_1	0.0703	mV^{-1}
ρ	0.309	-

Table S2: **Parameters for calculating Ca^{2+} at the BK$_{Ca}$ channel taken from (2).**

Parameter	Value	Unit
r	13	nm
D_{Ca}	250	μm^2 s^{-1}
F	9.6485	C mol^{-1}
k_B	500	μM^{-1} s^{-1}
B_{total}	30	μM
V_{Ca}	60	mV
$\bar{g}_{Ca}$	2.8	pS

1.1 Monte Carlo Simulations

We perform Monte Carlo simulations for the devised complex in order to model its stochastic gating. Initially the CaV and BK_{Ca} channels are closed. Then, for both the channels, the transitions from one state (closed, open or inactivated for CaV, closed or open for BK_{Ca}) to the others are given by the procedure explained below. First, we define the transition matrices for the CaV,

$$Q_{CaV} = \begin{bmatrix} P[C,t+\Delta t|C,t] & P[C,t+\Delta t|O,t] & 0 \\ P[O,t+\Delta t|C,t] & P[O,t+\Delta t|O,t] & P[O,t+\Delta t|B,t] \\ 0 & P[B,t+\Delta t|O,t] & P[B,t+\Delta t|B,t] \end{bmatrix}$$

$$= \begin{bmatrix} 1-\alpha\Delta t & \beta\Delta t & 0 \\ \alpha\Delta t & 1-\beta\Delta t-\delta\Delta t & \gamma\Delta t \\ 0 & \delta\Delta t & 1-\gamma\Delta t \end{bmatrix} ,$$

(S2)

and for the BK channel,

$$Q_{BK_{Ca}} = \begin{bmatrix} P[X,t+\Delta t|X,t] & P[X,t+\Delta t|Y,t] \\ P[Y,t+\Delta t|X,t] & P[Y,t+\Delta t|Y,t] \end{bmatrix}$$

$$= \begin{bmatrix} 1-k^+\Delta t & k^-\Delta t \\ k^+\Delta t & 1-k^-\Delta t \end{bmatrix}$$

(S3)

where the elements correspond to the transition probabilities between the indicated states in the time interval $[t, t+\Delta t]$, provided that Δt is small.

At any time point, we compute the state of the BK_{Ca}-CaV complex according the following procedure. We choose a random number ξ uniformly distributed on the interval $[0,1]$ for the CaV channel, and make a transition based upon the subinterval in which ξ falls. For example, if the CaV channel is open (O) (see the second column of Q_{CaV} defined by Eq. S2), it remains open if $\xi < 1-\beta\Delta t-\delta\Delta t$, while a transition to the inactivated (B) state occurs if $\xi \geq 1-\beta\Delta t-\delta\Delta t$ and $\xi < 1-\beta\Delta t$, otherwise ($\xi \geq 1-\beta\Delta t$ and $\xi \leq 1$) a transition to the closed (C) state occurs. Similarly, we choose a random number η uniformly distributed on the interval $[0,1]$ for the BK_{Ca} channel, and make a transition based upon the subinterval in which η falls. Note that the Ca^{2+} concentration for the BK_{Ca} channel at any time point is determined by the state of the CaV channel. This procedure is repeated for every time point to achieve the Monte Carlo simulations. We used $\Delta t = 0.01$ ms. Smaller time steps were checked and gave identical results.

1.2 Time to first opening and phase-type distributions

The continuous-time Markov chain Z in Figure 1A in the main text takes values in the state space $S = \{CX, OX, BX, BY, CY, OY\}$. We denote its initial distribution by λ and its generating matrix by Q, where

$$Q = \begin{bmatrix} -\alpha-k_c^+ & \alpha & 0 & 0 & k_c^+ & 0 \\ \beta & -\beta-\delta-k_o^+ & \delta & 0 & 0 & k_o^+ \\ 0 & \gamma & -\gamma-k_c^+ & k_c^+ & 0 & 0 \\ 0 & 0 & k_c^- & -\gamma-k_c^- & 0 & \gamma \\ k_c^- & 0 & 0 & 0 & -\alpha-k_c^- & \alpha \\ 0 & k_o^- & 0 & \delta & \beta & -\beta-\delta-k_o^- \end{bmatrix}.$$
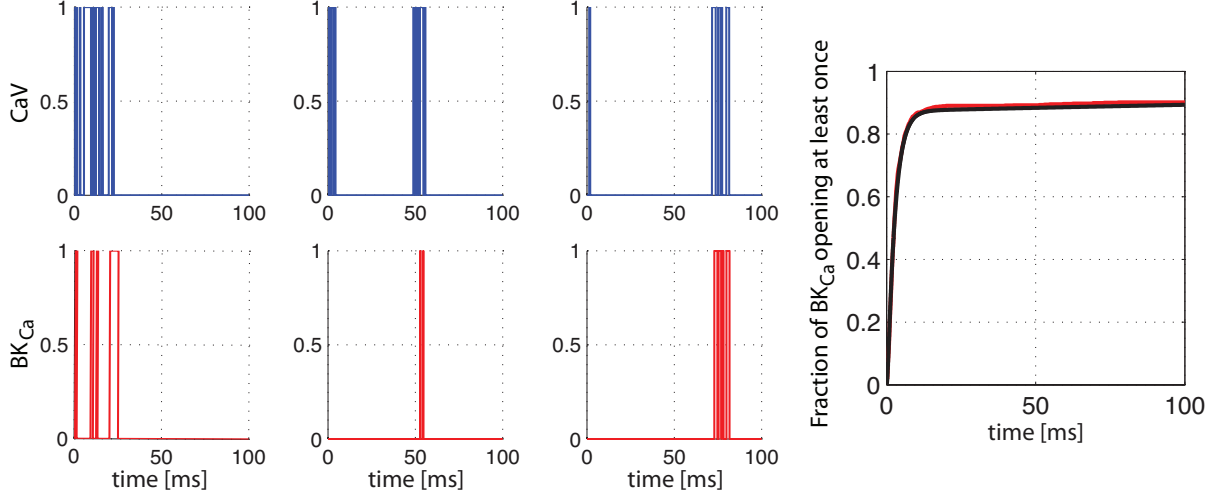
5

Figure S2: **Time to first opening for the 1:1 BK$_{\text{Ca}}$-CaV complex**. Left: Three Markov chain realizations for the 1:1 BK$_{\text{Ca}}$-CaV complex. Right: The empirical fraction of BK$_{\text{Ca}}$ channels that exhibit the first channel opening before t (red) and the theoretical expression $P(T_{CX,Y} < t)$ (black) from Eq. 22 of the main text. Note that in the second and third examples of Markov chain realizations, the CaV inactivates early before the BK$_{\text{Ca}}$ channel opens, and only later when the CaV reactivates (at $\sim$50 ms and $\sim$70 ms) does the BK$_{\text{Ca}}$ open for the first time. Such cases cause the late, slowly rising phase in the right panel, whereas the more typical case where the BK$_{\text{Ca}}$ channel opens early (as in the first example shown on the left) creates the rapid early rise in the right panel.

Assuming that $k_c^+ = 0$, the generating matrix Q become

$$Q = \begin{bmatrix} -\alpha & \alpha & 0 & 0 & 0 & 0 \\ \beta & -\beta - \delta - k_o^+ & \delta & 0 & 0 & k_o^+ \\ 0 & \gamma & -\gamma & 0 & 0 & 0 \\ 0 & 0 & k_c^- & -\gamma - k_c^- & 0 & \gamma \\ k_c^- & 0 & 0 & 0 & -\alpha - k_c^- & \alpha \\ 0 & k_o^- & 0 & \delta & \beta & -\beta - \delta - k_o^- \end{bmatrix}. \tag{S4}$$

Define the random variable

$$H = \inf\{t \geq 0 : Z_t \in \{CY, OY, BY\}\}, \tag{S5}$$

i.e., the (random) time to first opening, which can be described with phase-type distribution theory (5). We are interested in evaluating its conditional distribution and expectation, given that $Z_0 = CX$, i.e., with the initial distribution $\lambda = (1, 0, 0, 0, 0, 0)$. Defined $S_0 = \{CX, OX, BX, BY, CY\}$ and the matrix $\overline{Q} = (q_{i,j})_{i,j \in S_0}$, a simple application of phase-type distribution theory yields Eqs. 21 and 22 of the main text, as shown in "Time to first opening" in the Results section. Figure S2 shows that the simulated first opening times are well described by Eq. 22 of the main text.

2 Time-scale analysis and model simplifications

2.1 ODE model of the 1:1 BK_{Ca}-CaV complex

The deterministic description of the complex, corresponding to the Markov Chain described above, is given by the following ODE system

$$\frac{dp_{CX}}{dt} = k_c^- p_{CY} + \beta p_{OX} - (k_c^+ + \alpha)p_{CX}, \tag{S6}$$

$$\frac{dp_{CY}}{dt} = k_c^+ p_{CX} + \beta p_{OY} - (k_c^- + \alpha)p_{CY}, \tag{S7}$$

$$\frac{dp_{OX}}{dt} = k_o^- p_{OY} + \alpha p_{CX} + \gamma p_{BX} - (k_o^+ + \beta + \delta)p_{OX}, \tag{S8}$$

$$\frac{dp_{OY}}{dt} = k_o^+ p_{OX} + \alpha p_{CY} + \gamma p_{BY} - (k_o^- + \beta + \delta)p_{OY}, \tag{S9}$$

$$\frac{dp_{BX}}{dt} = k_c^- p_{BY} + \delta p_{OX} - (k_c^+ + \gamma)p_{BX}, \tag{S10}$$

$$\frac{dp_{BY}}{dt} = k_c^+ p_{BX} + \delta p_{OY} - (k_c^- + \gamma)p_{BY}, \tag{S11}$$

where p_Z, with $Z \in \{CX, CY, OX, OY, BX, BY\}$, represents the probability of the complex to be in one of the six states of the model. Then $p_Y = p_{CY} + p_{OY} + p_{BY}$. In the following, we assume $k_c^+ = 0$.

2.2 Model simplification

As explained in the Results section, since re- and inactivation of CaVs are slower than (de-)activation, the ODE model defined by Eqs. S6–S11 can be split into two submodels with respectively 4 and 2 states (the green and blue boxes in Figure 1A in the main text). Then, by considering only the activation of the BK_{Ca}-CaV complexes with non-inactivated CaV, and exploiting the relations $p_{CY} + p_{OY} = m_{BK}$, $p_{OX} + p_{OY} = m_{CaV}$, and $p_{CX} + p_{CY} = 1 - m_{CaV}$, where m_{BK} and m_{CaV} are the BK_{Ca} and the CaV activation variables, respectively, BK_{Ca} activation can be modeled by the two following ODEs,

$$\frac{dp_{CY}}{dt} = \beta m_{BK} - (k_c^- + \alpha + \beta)p_{CY}, \tag{S12}$$

$$\frac{dm_{BK}}{dt} = m_{CaV}k_o^+ + \left(k_o^+ + k_o^- + \alpha + \beta\right)p_{CY} - (k_o^+ + k_o^- + \beta)m_{BK}, \tag{S13}$$

with m_{CaV} modeled by Eq. 18 of the main text. Assuming quasi-steady state for p_{CY} ($\frac{dp_{CY}}{dt} \approx 0$) then yields

$$p_{CY} = \frac{\beta}{k_c^- + \alpha + \beta}m_{BK}. \tag{S14}$$

By substituting Eq. S14 into Eq. S13, we achieve a single ODE describing the dynamics of BK_{Ca} activation in complexes with non-inactivated CaV,

$$\frac{dm_{BK}}{dt} = m_{CaV}k_o^+ - \frac{(k_o^+ + k_o^-)(k_c^- + \alpha) + \beta k_c^-}{\alpha + \beta + k_c^-}m_{BK}. \tag{S15}$$
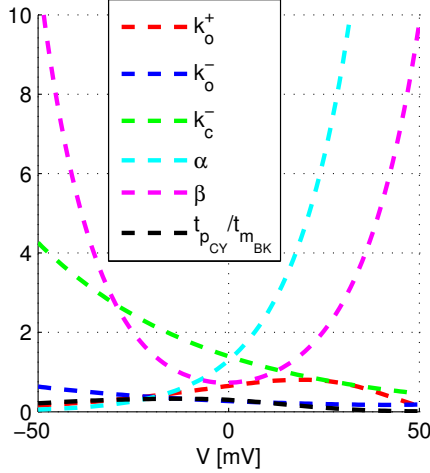
Figure S3: **Time scale analysis for the 1:1 BK$_{\text{Ca}}$-CaV complex**. Model parameters as function of voltage, showing that the transitions described by α, β and k_c^- are the fastest. This fact leads to a separation of time scales, as shown by the black curve illustrating $t_{p_{CY}}/t_{m_{BK}}$ in Eq. S18, which is always less than 0.33, and for most voltages considerably smaller.

Therefore, the equilibrium open fraction of the BK$_{\text{Ca}}$ channels in complexes with non-inactivated CaV, $m_{BK,\infty}$, and the corresponding time constant, τ_{BK}, are given as in Eq. 24 of the main text.

Coupling the one state model for the BK$_{\text{Ca}}$ activation (Eq. S15) with the inactivation of the CaV channel allows us to reproduce the dynamics of the BK$_{\text{Ca}}$-CaV complex described by Eqs. S6–S11 and the corresponding Monte Carlo simulations (see Figure 1 in the main text). In particular, the open probability of the BK$_{\text{Ca}}$ channel, $p_Y = p_{CY} + p_{OY} + p_{BY}$, can be described by

$$p_Y \approx m_{BK}h, \tag{S16}$$

where h is the fraction of non-inactivated CaV (see Eqs. 15 and 20 of the main text).

2.3 Time scale analysis

For a more formal analysis, we follow (6). The quasi-steady state approximation for p_{CY} is valid when the time scales of the two variables in question differ, i.e., $t_{p_{CY}} \ll t_{m_{BK}}$, where $t_{m_{BK}}$ is the time scale of changes m_{BK} after an initial (fast) transient, i.e., when the approximation is consistent (6). The (fast) time scale for p_{CY} is given from Eq. S12, assuming that m_{BK} is constant, as

$$t_{p_{CY}} = \frac{1}{\alpha + \beta + k_c^-} \ . \tag{S17}$$

The (slow) time scale for m_{BK} is given as the time scale of m_{BK} assuming that the quasi-steady state approximation holds, i.e., $t_{m_{BK}} = \tau_{BK}$ in Eq. 24 of the main text. Then

$$\frac{t_{p_{CY}}}{t_{m_{BK}}} = \frac{(k_o^- + k_o^+)(k_c^- + \alpha) + \beta k_c^-}{(\alpha + \beta + k_c^-)^2}, \tag{S18}$$
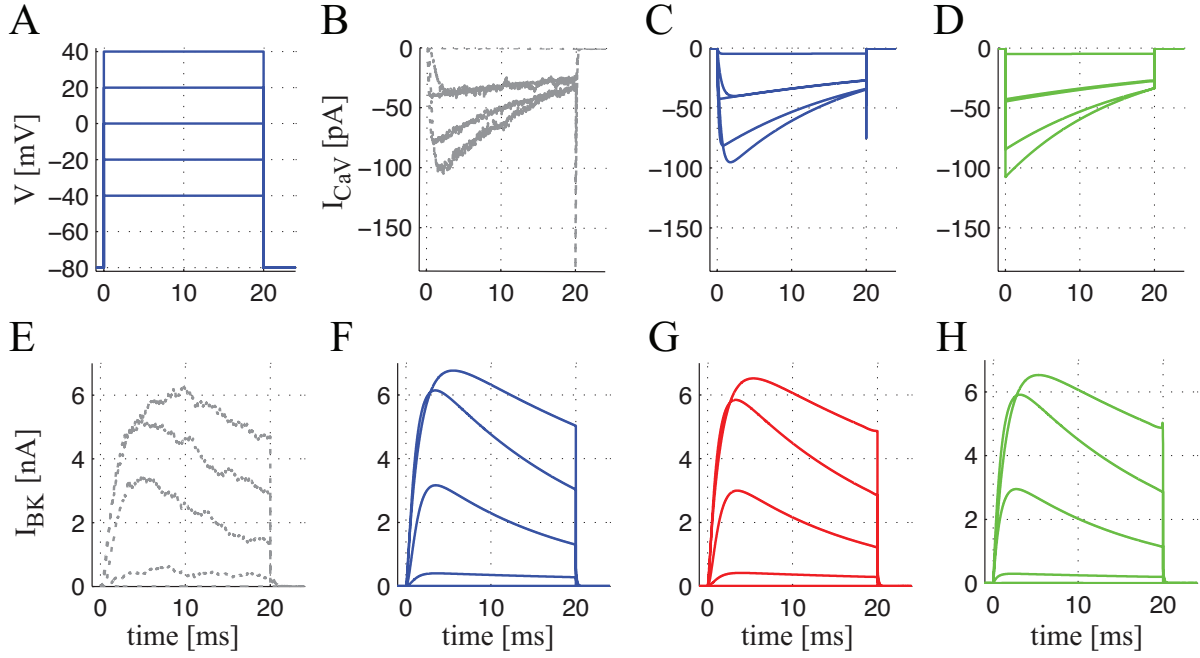
which is small (Figure S3).

Figure S4: **Model responses to different voltage steps for the 1:1 BK$_{Ca}$-CaV complex**.
(**A**) Voltage steps from -80 mV to from -40 mV to 40 mV in 20 mV increments for 20 ms and then
back to -80 mV. Simulated CaV currents in response to the different voltage steps obtained from
(**B**) the 7-state Markov chain model (see (2); gray), (**C**) the ODE model corresponding to the 3-
state Markov chain model (Eqs. 13-15 of the main text; blue), and (**D**) the corresponding model
assuming instantaneous activation $m_{CaV} = m_{CaV,\infty}$ (Eq. 20 of the main text; green). Simulated
BK$_{Ca}$ currents in response to the different voltage steps obtained from (**E**) the original 70-state
Markov chain model (see (2); gray), (**F**) the ODE model corresponding to the 6-state Markov
chain model (Eqs. S19–S24; blue), (**G**) the simplified Hodgkin-Huxley-type model (Eq. 25 of the
main text; red), and (**H**) the corresponding model assuming instantaneous activation $m_{CaV} = m_{CaV,\infty}$ (green; see main text). Each trace is the sum of 1000 single complex responses.
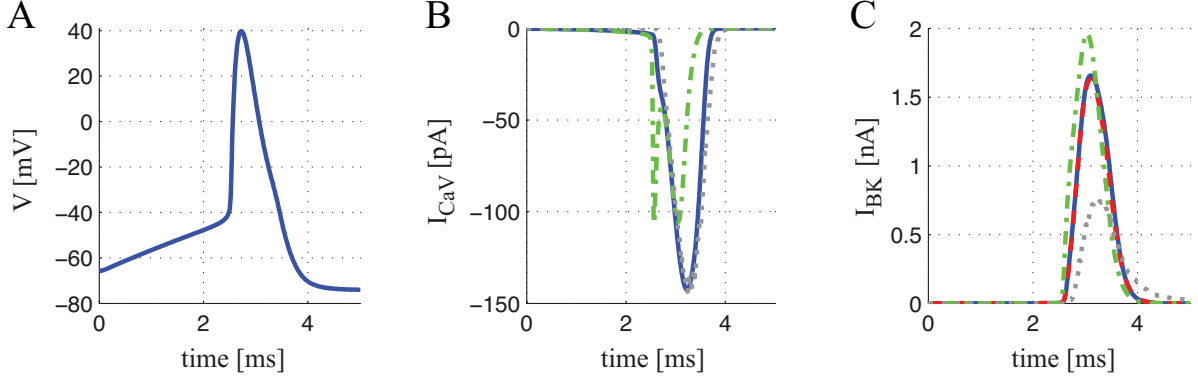
9

Figure S5: **Model responses to a simulated AP generated by a model of hypothalamic neurosecretory cells (7)**. **(A)** Simulated AP. **(B)** Simulated CaV currents in response to the simulated AP obtained from the 7-state Markov chain model ((2); dotted gray), the ODE model corresponding to the 3-state Markov chain model (Eqs. 13-15 of the main text; solid blue), and the corresponding model assuming instantaneous activation $m_{CaV} = m_{CaV,\infty}$ (Eq. 20 of the main text; dash-dotted green). **(C)** Simulated BK$_{Ca}$ currents in response to the simulated AP obtained from the original 70-state Markov chain model ((2); gray), the ODE model corresponding to the 6-state Markov chain model (Eqs. S19–S24; solid blue), the simplified Hodgkin-Huxley-type model (Eq. 25 of the main text; dashed red), and the corresponding model assuming instantaneous activation $m_{CaV} = m_{CaV,\infty}$ (dash-dotted green; see main text). Each trace is the sum of 1000 single complex responses.

2.4   Responses of the 1:1 BK$_{Ca}$-CaV complex to voltage steps and AP

Figure S4 shows the current response of the 1:1 BK$_{Ca}$-CaV complex to different step voltages (Figure S4A). The whole-cell CaV current for the 3-state ODE model ($I_{CaV} = N_{CaV}\bar{g}_{Ca}m_{CaV}h$, where $N_{CaV} = 1000$ is the number of CaV channels, $\bar{g}_{Ca}$ is defined in Table S2 and m_{CaV} and h are given by Eqs. 13-18 of the main text) approximates the 7-state Markov chain model (2) current very well for each step voltage (Figure S4BC). Also, the further simplification for the 3-state ODE model assuming instantaneous activation of the CaV currents ($m_{CaV} = m_{CaV,\infty}$, green plots in Figure S4D) provides a good approximation of the Monte Carlo simulations. The whole-cell BK$_{Ca}$ current for our simplified 6-state Markov chain model ($I_{BK} = N_{BK}\bar{g}_{BK}p_Y$, where $N_{BK} = 1000$ is the number of BK$_{Ca}$ channels, $\bar{g}_{BK} = 100$ pF is the single BK$_{Ca}$ channel conductance (8) and p_Y is given by Eqs. S19-S24) approximates the 70-state Markov chain model (2) current very well for each step voltage (Figure S4EF). Moreover, our simplified Hodgkin-Huxley-type model current for the BK$_{Ca}$ channel (Eq. 25 of the main text; red plots in Figure S4G), and the corresponding model assuming instantaneous activation of the CaV currents (green plots in Figure S4H) also works very well.

Figure S5 shows the current response of the 1:1 BK$_{Ca}$-CaV complex to a simulated action potential (AP) generated by a model of hypothalamic neurosecretory cells (7) (Figure S5A). As for the voltage step response case, the whole-cell CaV current for the 3-state ODE model approximates the 7-state Markov chain model current very well (see solid blue and dotted gray plots in Figure S5B). However, the further simplification for the 3-state ODE model assuming instantaneous activation of the CaV currents (dash-dotted green plot in Figure S5B) determines an additional early peak of current and a faster decay. For the whole-cell BK$_{Ca}$ current, the peak obtained from the 70-state Markov chain model is lower than that obtained from our simplified

10

models (Figure S5C). This discrepancy is likely due to an overestimation of the BK_{Ca} activation time constant of BK_{Ca} model devised by Cox (2) at specific Ca_o (compare the left lower panel of Figure 2D in (2) with Figure S1D, where $Ca_o = 22\ \mu M$). The slower time constant prevents complete activation of the BK_{Ca} channels for Cox' 70-state Markov chain model during the imposed AP.

3 Model for BK_{Ca} activation in complexes with k non-inactivated CaVs and its approximation

For the case of 1:n BK_{Ca}-CaV stoichiometry, we split the system according to the number k of non-inactivated CaV channels. Then the equivalent 1:k BK_{Ca}-CaV complex can be described by the following ODE system:

$$\frac{dp_{C_kX}}{dt} = \beta p_{C_{k-1}OX} + k_c^- p_{C_kY} - (k\alpha + k_c^+)p_{C_kX} \tag{S19}$$

$$\frac{dp_{C_kY}}{dt} = \beta p_{C_{n-1}OY} + k_c^+ p_{C_nX} - (k\alpha + k_c^-)p_{C_nY} \tag{S20}$$

$$\frac{dp_{C_{k-i}O_iX}}{dt} = (i+1)\beta p_{C_{k-(i+1)}O_{i+1}X} + (k-(i-1))\alpha p_{C_{k-(i-1)}O_{i-1}X}$$
$$+ k_{oi}^- p_{C_{k-i}O_iY} - ((k-i)\alpha + i\beta + k_{oi}^+)p_{C_{k-i}O_iX}, \quad i = 1,\dots,k-1 \tag{S21}$$

$$\frac{dp_{C_{k-i}O_iY}}{dt} = (i+1)\beta p_{C_{n-(i+1)}O_{i+1}Y} + (k-(i-1))\alpha p_{C_{k-(i-1)}O_{i-1}Y}$$
$$+ k_{oi}^+ p_{C_{k-i}O_iX} - ((k-i)\alpha + i\beta + k_{oi}^-)p_{C_{k-i}O_iY}, \quad i = 1,\dots,k-1 \tag{S22}$$

$$\frac{dp_{O_kX}}{dt} = \alpha p_{CO_{k-1}X} + k_{ok}^- p_{O_kY} - (k\beta + k_{ok}^+)p_{O_kX} \tag{S23}$$

$$\frac{dp_{O_kY}}{dt} = \alpha p_{CO_{k-1}Y} + k_{ok}^+ p_{O_kX} - (k\beta + k_{ok}^-)p_{O_kY} \tag{S24}$$

where, e.g., $p_{C_{k-i}O_iX}$ and $p_{C_{k-i}O_iY}$ correspond to the probability of having $k-i$ closed and i open CaVs coupled with the closed (X) and open (Y) BK_{Ca} channel, respectively. The activation of the BK_{Ca} surrounded by k non-inactivated CaVs, $m_{BK}^{(k)}$, is then

$$m_{BK}^{(k)} = p_{C_kY} + \sum_{i=1}^{k-1} p_{C_{k-i}O_iY} + p_{O_kY}. \tag{S25}$$

By taking into account that

$$p_{C_kX} = (1-m_{CaV})^k - p_{C_kY} \tag{S26}$$

$$p_{C_{k-i}O_iX} = \binom{k}{i}(1-m_{CaV})^{k-i}m_{CaV}^i - p_{C_{k-i}O_iY}, \quad i = 1,\dots,k-1 \tag{S27}$$

$$p_{O_kX} = m_{CaV}^k - p_{O_kY} \tag{S28}$$

and renaming the state variables as follows

$$p_{Y_0} = p_{C_k Y} \tag{S29}$$

$$p_{Y_1} = p_{C_{k-1}O_Y} + p_{Y_0} \tag{S30}$$

$$\vdots$$

$$p_{Y_i} = p_{C_{k-i}O_i Y} + p_{Y_{i-1}} \tag{S31}$$

$$\vdots$$

$$m_{BK}^{(k)} = p_{Y_k} = p_{O_k Y} + p_{Y_{k-1}} \tag{S32}$$

we can reduce the ODE system from $2(k+1)$ to $(k+1)$ equations.

Moreover, assuming the quasi-steady state approximation for p_{Y_i}, with $i = 0, \ldots, k-1$,

$$\frac{dp_{Y_i}}{dt} = 0,$$

then

$$p_{Y_0} = A_1 p_{Y_1} + D_1 \tag{S33}$$

$$\vdots$$

$$p_{Y_i} = A_{i+1} p_{Y_{i+1}} + D_{i+1} \tag{S34}$$

$$\vdots$$

$$p_{Y_{k-1}} = A_k m_{BK}^{(k)} + D_n \tag{S35}$$

where (for brevity, $m = m_{CaV}$)

$$A_1 = \frac{\beta}{k\alpha + \beta + k_c^- + k_c^+} \cong \frac{\beta}{k\alpha + \beta + k_c^-}$$

$$D_1 = \frac{k_c^+ (1-m)^k}{k\alpha + \beta + k_c^- + k_c^+} \cong 0$$

$$A_i = \frac{i\beta}{B_i}, \qquad i = 2, \ldots, k$$

$$D_i = \left(\sum_{j=1}^{i-1} \binom{k}{j} (1-m)^{k-j} m^j - k_c^- \left(D_1 + \sum_{j=2}^{i-1} D_j \left(\prod_{l=1}^{j-1} A_l \right) \right) \right) / B_i$$

$$\left(-\sum_{j=1}^{i-2} \left(k_{oj}^+ + k_{oj}^- \right) \left((1 - A_j) \left(D_{j+1} + \sum_{l=j+2}^{i-1} D_l \left(\prod_{m=j+1}^{l-1} A_m \right) \right) - D_j \right) \right) / B_i$$

$$\left(+ \left((k - (i-1)) \alpha + k_{o(i-1)}^+ + k_{o(i-1)}^- \right) D_{i-1} \right) / B_i, \quad i = 2, \ldots, k$$

with

$$B_i = \left((k - (i-1)) \alpha + k_{o(i-1)}^+ + k_{o(i-1)}^- \right) (1 - A_{i-1}) + i\beta + k_c^- \left(\prod_{j=1}^{i-1} A_j \right)$$

$$+ \sum_{j=1}^{i-2} \left(k_{oj}^+ + k_{oj}^- \right) (1 - A_j) \left(\prod_{l=j+1}^{i-1} A_l \right), \quad i = 2, \ldots, k.$$

Then

$$p_{Y_i} = \left(\prod_{j=1}^{k} A_j\right) m_{BK}^{(k)} + D_{i+1} + \sum_{j=i+2}^{k} D_j \left(\prod_{l=i}^{j-1} A_l\right), \ i = 0, \ldots, k-1$$

$$p_{C_k Y} = \left(\prod_{j=1}^{k} A_j\right) m_{BK}^{(k)} + D_1 + \sum_{j=2}^{k} D_j \left(\prod_{l=1}^{j-1} A_l\right)$$

$$p_{C_{k-i} O_i Y} = (1 - A_i) \left(\prod_{j=i+1}^{k} A_j\right) m_{BK}^{(k)} + (1 - A_i) \left(D_{i+1} + \sum_{j=i+2}^{k} D_j \left(\prod_{l=i+1}^{j-1} A_l\right)\right)$$
$$- D_i, \quad i = 1, \ldots, k-1$$

$$p_{O_k Y} = (1 - A_k) m_{BK}^{(k)} - D_k.$$

Finally, we achieve one ODE for describing the dynamics of the BK_{Ca} activation with k non-inactivated CaVs:

$$\frac{dm_{BK}^{(k)}}{dt} = \sum_{i=1}^{k} \binom{k}{i}(1-m)^{k-i}m^i k_{oi}^+ - k_c^- p_{C_k Y} - \sum_{i=1}^{k} \left(k_{oj}^+ + k_{oj}^-\right) p_{C_{k-i} O_i Y}$$

$$= \left\{ \sum_{i=1}^{k} \binom{k}{i}(1-m)^{k-i}m^i k_{oi}^+ - k_c^- \left(D_1 + \sum_{j=2}^{k} D_j \left(\prod_{l=1}^{j-1} A_l\right)\right) \right.$$

$$- \sum_{i=1}^{k-1} \left(k_{oj}^+ + k_{oj}^-\right) \left((1 - A_i) \left(D_{i+1} + \sum_{j=i+2}^{k} D_j \left(\prod_{l=i+1}^{j-1} A_l\right)\right) - D_i\right)$$

$$\left. + \left(k_{ok}^+ + k_{ok}^-\right) D_n \right\} \tag{S36}$$

$$- \left[\left(k_{ok}^+ + k_{ok}^-\right)(1 - A_k) + k_c^- \prod_{j=1}^{k} A_j + \sum_{i=1}^{k-1} \left(k_{oj}^+ + k_{oj}^-\right)(1 - A_i) \prod_{j=i+1}^{k} A_j\right] m_{BK}^{(k)}.$$

Therefore, the activation time constant of the BK_{Ca} channels in complexes with k non-inactivated CaVs, $\tau_{BK}^{(k)}$, is the inverse of the expression in square brackets in Eq. S36, whereas the BK_{Ca} equilibrium open fraction, $m_{BK,\infty}^{(k)}$, is equal to the product of $\tau_{BK}^{(k)}$ and the expression in curly brackets. Note that $\tau_{BK}^{(k)}$ depends only on parameters, whereas $m_{BK}^{(k)}$ depends also on m_{CaV} via D_i.

If assuming instantaneous activation of CaVs, we have

$$p_{C_{k-i} O_i Y} = \binom{k}{i}(1 - m_{CaV,\infty})^{k-i} m_{CaV,\infty}^i p_Y, \quad i = 0, \ldots, k,$$

and (cf. Eq. 29 of the main text)

$$
\begin{aligned}
\frac{dm_{BK}^{(k)}}{dt} &= \sum_{i=1}^{k} \binom{k}{i} (1 - m_{CaV,\infty})^{n-i} m_{CaV,\infty}^{i} k_{io}^{+} - k_{c}^{-} p_{C_{k}Y} - \sum_{i=1}^{k} \left(k_{oj}^{+} + k_{oj}^{-} \right) p_{C_{k-i}O_{i}Y} \\
&= \sum_{i=1}^{k} \binom{k}{i} (1 - m_{CaV,\infty})^{k-i} m_{CaV,\infty}^{i} k_{oi}^{+} \\
&\quad - \left((1 - m_{CaV,\infty})^{k} k_{c}^{-} + \sum_{i=1}^{k} \binom{k}{i} (1 - m_{CaV,\infty})^{k-i} m_{CaV,\infty}^{i} \left(k_{oi}^{+} + k_{oi}^{-} \right) \right) m_{BK}.
\end{aligned}
\tag{S37}
$$

4 Whole-cell models

4.1 Hypothalamic neuronal model

We extended a model of electrical activity in hypothalamic neurosecretory cells (7) with our devised BK_{Ca}-CaV model. The model is described by

$$
\frac{dV}{dt} = -\frac{1}{C} \left(I_{BK} + I_{SK} + I_{K} + I_{A} + I_{Na} + I_{Ca} + I_{leak} \right).
\tag{S38}
$$

where I_{BK} and I_{SK} represent the calcium- and voltage-dependent K^{+} currents carried by BK and SK channels, respectively; I_{K} and I_{A} denote the delayed rectifier and the A-current respectively; I_{Na} represents the sodium current and I_{Ca} the calcium current. C is the membrane capacitance and is equal to 1 $\mu F\,cm^{-2}$.

We modified the calcium current and inserted our whole-cell BK_{Ca} model in place of the original representation of BK_{Ca} currents. In particular, according to experimental data (9, 10), we introduced CaV activation dynamics, whereas the original model assumed instantaneous activation of CaVs, and modified the equilibrium voltage-dependent activation. Then

$$
I_{Ca} = g_{Ca} m_{CaV} (V - V_{Ca})
\tag{S39}
$$

where g_{Ca} and V_{Ca} are the maximal whole-cell conductance and the Ca^{2+} reverse potential, respectively (7). m_{CaV} is defined by Eq. 18 of the main text, with $\tau_{CaV} = 1.25$ ms. For the equilibrium voltage-dependent activation, given in (7) and defined by $m_{CaV,\infty} = \left(1 + e^{\frac{-V-V_m}{k_m}} \right)^{-1}$, we modified the V_m parameter of the Boltzmann function ($V_m = 15$ mV).

The I_{BK} current is modeled by Eq. 28 of the main text, where the BK_{Ca} activation, $m_{BK}^{(n)}$, is given by Eq. 26. Moreover, we also considered the case where the activation of the BK_{Ca} channel is given by the complete ODE model described by Eqs. S19–S25, and the case where the BK_{Ca} activation is simplified by assuming instantaneous activation of CaVs (see Eq. S37 and Eq. 29 of the main text).

The other currents are expressed as (7)

$$
I_{SK} = g_{SK} q_{\infty}^{2} (V - V_{K}),
\tag{S40}
$$

$$
I_{K} = g_{K} m_{K}^{3} (V - V_{K}),
\tag{S41}
$$

$$
I_{A} = g_{A} m_{A}^{4} h_{A} (V - V_{K}),
\tag{S42}
$$

$$
I_{Na} = g_{Na} [m_{Na,\infty}(V)]^{3} h_{Na} (V - V_{Na}),
\tag{S43}
$$

$$
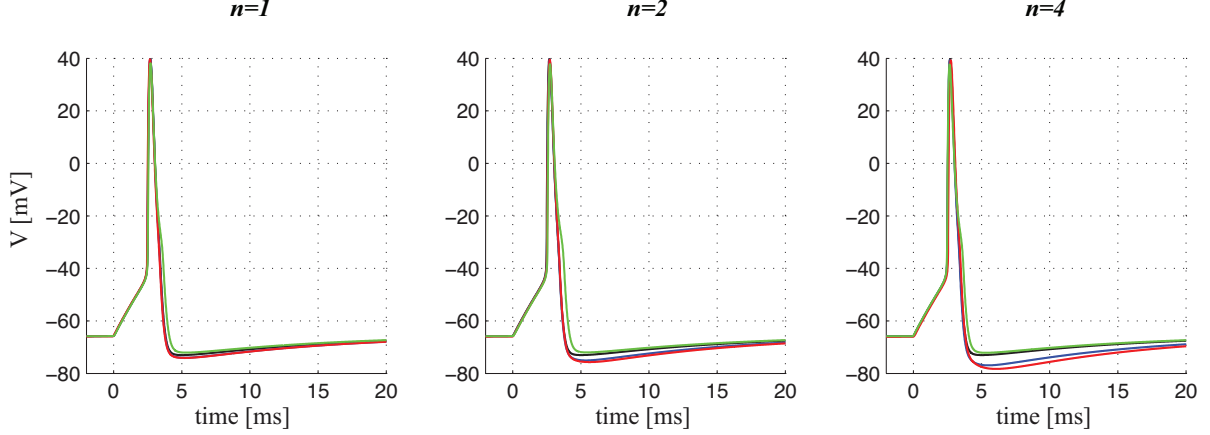I_{leak} = g_{leak} (V - V_{leak}),
\tag{S44}
$$

Figure S6: **Whole-cell simulations for the neuronal model (7) with the devised BK_{Ca}-CaV model**. Simulated APs with the BK_{Ca} channels coupled in complexes with n non-inactivating CaVs ($n = 1$, left panel; $n = 2$, middle; $n = 4$, right). In each panel, the whole-cell BK_{Ca} current is described by Eq. 28 of the main text (i.e. BK_{Ca} coupled with non-inactivating CaVs), where the BK_{Ca} activation, $m_{BK}^{(n)}$, is modeled by the full ODE model described by Eqs. S19–S25 (blue curve), by Eq. 26 (see Eq. S36 for the details) (red curve), and by Eq. 29 (green curve), and $g_{BK} = 1$ mS cm^{-2}. The black curve shows the case of BK_{Ca} block ($g_{BK} = 0$ mS cm^{-2}).

where the voltage-dependent activation variables, m_X (and similarly inactivation variabels, h_X, where X denotes the type of current), follow

$$\frac{dm_X}{dt} = \frac{m_{X,\infty}(V) - m_X}{\tau_{mX}}, \tag{S45}$$

where τ_{mX} (respectively τ_{hX}) is the time-constant of activation (respectively inactivation for h_X), and $m_{X,\infty}(V)$ (respectively $h_{X,\infty}(V)$) is the steady-state voltage-dependent activation (respectively inactivation) of the current, described with Boltzmann function. g_X represents the whole-cell conductance of the channel X and V_X the reverse potential. q_∞ is the calcium-dependent activation function for I_{SK} (see Appendix in (7) for parameter values).

Figure S6 shows the simulated AP in this neuronal model with 1:n stoichiometry BK_{Ca}-CaV complexes, where $n = 1$, 2 or 4. The BK_{Ca} activation is modeled by the complete ODE system described by Eqs. S19–S25, by Eq. 26 of the main text, or by Eq. 29. The simplified model (Eq. 29) is not able to reproduce the fast after-hyperpolarization (fAHP), whereas the other two models, which take CaV activation dynamics into account, show how increasing the number of CaVs coupled with BK_{Ca} helps to generate fAHP. The difference associated with the choice of the BK_{Ca} model suggests that the neuronal model is sensitive to the kinetics of BK_{Ca} activation.

4.2 Human β-cell model

The human β-cell model (11) is as follows. The membrane potential is described by

$$\frac{dV}{dt} = -(I_{BK} + I_{Kv} + I_{HERG} + I_{Na} + I_{CaL} + I_{CaPQ} + I_{CaT} + I_{KATP} + I_{leak}), \qquad \text{(S46)}$$

where the BK_{Ca} current I_{BK} is modeled assuming that BK_{Ca} channels are located in complexes with either T-type, L-type or P/Q-type Ca^{2+} channels. In particular, I_{BK} is described by Eq. 27 of the main text (with inactivating T- and L-type CaVs) or Eq. 28 (with non-inactivating P/Q-type CaVs), where the BK_{Ca} activation, $m_{BK}^{(n)}$, is modeled by Eqs. S19–S25 (full model), Eq. 26, or Eq. 29 (instantaneous CaV activation). As shown in Figure S7, the model is quite robust to the choice of BK_{Ca}-CaV model.

The other currents are

$$I_{Kv} = g_{Kv} m_{Kv}(V - V_K), \qquad \text{(S47)}$$

$$I_{HERG} = g_{HERG} m_{HERG} h_{HERG}(V - V_K), \qquad \text{(S48)}$$

$$I_{Na} = g_{Na} m_{Na,\infty}(V) h_{Na}(V - V_{Na}), \qquad \text{(S49)}$$

$$I_{CaL} = g_{CaL} m_{CaL,\infty}(V) h_{CaL}(V - V_{Ca}), \qquad \text{(S50)}$$

$$I_{CaPQ} = g_{CaPQ} m_{CaPQ,\infty}(V)(V - V_{Ca}), \qquad \text{(S51)}$$

$$I_{CaT} = g_{CaT} m_{CaT,\infty}(V) h_{CaT}(V - V_{Ca}), \qquad \text{(S52)}$$

$$I_{K(ATP)} = g_{K(ATP)}(V - V_K), \qquad \text{(S53)}$$

$$I_{leak} = g_{leak}(V - V_{leak}), \qquad \text{(S54)}$$

where activation variables (and similarly inactivations variabels, h_X, where X denotes the type of current) follow

$$\frac{dm_X}{dt} = \frac{m_{X,\infty}(V) - m_X}{\tau_{mX}}, \qquad \text{(S55)}$$

where τ_{mX} (respectively τ_{hX}) is the time-constant of activation (respectively inactivation for h_X), and $m_{X,\infty}(V)$ (respectively $h_{X,\infty}(V)$) is the steady-state voltage-dependent activation (respectively inactivation) of the current. The steady-state activation (and inactivation) functions are described with Boltzmann functions,

$$m_{X,\infty}(V) = \frac{1}{1 + \exp((V - V_{mX})/n_{mX})}, \qquad \text{(S56)}$$

except

$$h_{CaL,\infty}(V) = \max\left(0, \min\left\{1, 1 + [m_{CaL,\infty}(V)(V - V_{Ca})]/57\text{mV}\right\}\right), \qquad \text{(S57)}$$

for Ca^{2+}-dependent inactivation of L-type Ca^{2+} channels. The time-constant for activation of Kv-channes is assumed to be voltage-dependent (11, 12),

$$\tau_{mKv} = \begin{cases} \tau_{mKv,0} + 10\exp\left(\frac{-20\,\text{mV} - V}{6\text{mV}}\right)\ \text{ms}, & \text{for } V \geq 26.6\ \text{mV}, \\ \tau_{mKv,0} + 30\ \text{ms}, & \text{for } V < 26.6\ \text{mV}. \end{cases} \qquad \text{(S58)}$$

We refer to the original paper (11) for details regarding modeling of the different currents.
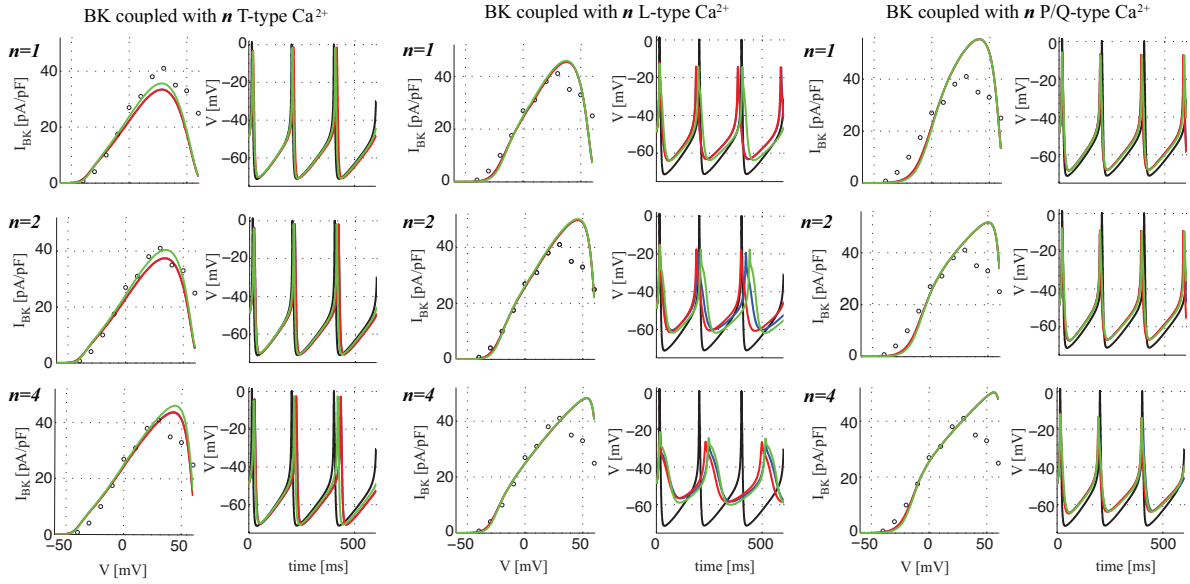
Figure S7: **Whole-cell simulations for the human β-cell model (11) with the devised BK$_{Ca}$-CaV model.** Simulated APs with BK$_{Ca}$ channels located in complexes with n T-type (left panels), L-type (middle), or P/Q-type (right) CaVs ($n = 1$, upper panels; $n = 2$, middle; $n = 4$, lower). The β-cell model shows little sensitivity to the choice of BK$_{Ca}$-CaV model. In each panel, the whole-cell BK$_{Ca}$ current is described by Eq. 27 of the main text (with inactivating T- and L-type CaVs) or Eq. 28 (with non-inactivating P/Q-type CaVs), where the BK$_{Ca}$ activation, $m_{BK}^{(n)}$, is modeled by the full ODE model described by Eqs. S19–S25 (blue curve), by Eq. 26 (see Eq. S36 for the details) (red curve), and by Eq. 29 (green curve). Left subpanels show fit to data from (12), right subpanels report model simulations. The black traces show simulations with BK$_{Ca}$ block.

4.3 Pituitary lactotroph model

We extended a pituitary lactotroph model (13) with our concise Hodgkin-Huxley-type model of the BK$_{\text{Ca}}$-CaV complex (Eq. 28 of the main text). The original model includes a single Ca^{2+} current (I_{Ca}), a delayed-rectifier K$^+$ current (I_K), a Ca^{2+}-gated SK current (I_{SK}), and a leak current (I_{leak}), in addition to the BK current. The membrane potential V evolves in time according to

$$C\frac{dV}{dt} = -(I_{Ca} + I_K + I_{SK} + I_{BK} + I_{leak}), \tag{S59}$$

where C is the membrane capacitance. The currents are modeled as

$$
\begin{aligned}
I_{Ca} &= g_{Ca}m_{CaV,\infty}(V)(V - V_{Ca}), & \text{(S60)}\\
I_K &= g_K n(V - V_K), & \text{(S61)}\\
I_{SK} &= g_{SK}s_\infty([Ca])(V - V_K), & \text{(S62)}\\
I_{leak} &= g_l(V - V_l), & \text{(S63)}\\
I_{BK} &= g_{BK}m_{BK}^{(n)}(V - V_K), & \text{(S64)}
\end{aligned}
$$

where the activation variable of the delayed rectifier is given by

$$\frac{dn}{dt} = \frac{n_\infty(V) - n}{\tau_n}. \tag{S65}$$

The equilibrium functions are described as

$$
\begin{aligned}
m_{CaV,\infty}(V) &= [1 + \exp((v_m - V)/s_m)]^{-1}, & \text{(S66)}\\
n_\infty(V) &= [1 + \exp((v_n - V)/s_n)]^{-1}, & \text{(S67)}\\
s_\infty([Ca]) &= \frac{[Ca]^2}{[Ca]^2 + k_s^2}. & \text{(S68)}
\end{aligned}
$$

The differential equation for the cytosolic Ca^{2+} concentration is

$$\frac{d[Ca]}{dt} = -f_c(\alpha I_{Ca} + k_c[Ca]). \tag{S69}$$

Table S3 reports the parameter values of the pituitary model (13).

Table S3: **Parameter values of the pituitary model (13)**.

Parameter	Value	Unit
C	10	pF
g_{Ca}	2	nS
V_{Ca}	60	mV
v_m	-20	mV
s_m	12	mV
g_k	3	nS
V_k	-75	mV
v_n	-5	mV
s_n	10	mV
g_{SK}	1.2	nS
k_s	0.4	μM
g_{BK}	1	nS
g_l	0.2	nS
V_l	-50	mV
f_c	0.01	-
α	0.0015	μM fC^{-1}
k_c	0.12	ms^{-1}

Supporting References

1. Cox, D. H., J. Cui, and R. W. Aldrich, 1997. Allosteric gating of a large conductance Ca-activated K+ channel. *J Gen Physiol* 110:257–81.

2. Cox, D. H., 2014. Modeling a Ca(2+) channel/BKCa channel complex at the single-complex level. *Biophys J* 107:2797–814.

3. Latorre, R., and S. Brauchi, 2006. Large conductance Ca2+-activated K+ (BK) channel: activation by Ca2+ and voltage. *Biol Res* 39:385–401.

4. Berkefeld, H., B. Fakler, and U. Schulte, 2010. Ca2+-activated K+ channels: from protein complexes to function. *Physiol Rev* 90:1437–59.

5. Buchholz, P., J. Kriege, and I. Felko, 2014. Input modeling with phase-type distributions and Markov models. Springer Briefs in Mathematics. Springer. http://dx.doi.org/10.1007/978-3-319-06674-5.

6. Segel, L. A., and M. Slemrod, 1989. The quasi steady-state assumption: a case study in perturbation. *SIAM Rev.* 31:446–477.

7. Roper, P., J. Callaway, T. Shevchenko, R. Teruyama, and W. Armstrong, 2003. AHP's, HAP's and DAP's: how potassium currents regulate the excitability of rat supraoptic neurones. *J Comput Neurosci* 15:367–89.

8. Pallotta, B. S., K. L. Magleby, and J. N. Barrett, 1981. Single channel recordings of Ca2+-activated K+ currents in rat muscle cell culture. *Nature* 293:471–4.

9. Joux, N., V. Chevaleyre, G. Alonso, L. Boissin-Agasse, F. C. Moos, M. G. Desarménien, and N. Hussy, 2001. High voltage-activated Ca2+ currents in rat supraoptic neurones: biophysical properties and expression of the various channel alpha1 subunits. *J Neuroendocrinol* 13:638–49.

10. Berkefeld, H., and B. Fakler, 2008. Repolarizing responses of BKCa-Cav complexes are distinctly shaped by their Cav subunits. *J Neurosci* 28:8238–45.

11. Pedersen, M. G., 2010. A biophysical model of electrical activity in human β-cells. *Biophys J* 99:3200–3207. http://dx.doi.org/10.1016/j.bpj.2010.09.004.

12. Braun, M., R. Ramracheya, M. Bengtsson, Q. Zhang, J. Karanauskaite, C. Partridge, P. R. Johnson, and P. Rorsman, 2008. Voltage-gated ion channels in human pancreatic beta-cells: electrophysiological characterization and role in insulin secretion. *Diabetes* 57:1618–1628. http://dx.doi.org/10.2337/db07-0991.

13. Tabak, J., N. Toporikova, M. E. Freeman, and R. Bertram, 2007. Low dose of dopamine may stimulate prolactin secretion by increasing fast potassium currents. *J Comput Neurosci* 22:211–22.